Discovering extragalactic high-mass X-ray binaries

Author: Marc Miguel Rivas, mmigueri11@alumnes.ub.edu
Facultat de Física, Universitat de Barcelona, Diagonal 645, 08028 Barcelona, Spain.

Advisors: Nadejda Blagorodnova, nblagorodnova@ub.edu; Hugo Tranin, htranin@icc.ub.edu

Abstract: This TFG presents a search for high-mass X-ray binaries (HMXBs) in M31 and M33 using Chandra X-ray data and Hubble Space Telescope (HST) optical data. Our selection crossmatches the two datasets, applies a selection cut based on the optical stellar mass and removes foreground contamination. This allows us to identify 18 HMXB candidates in M31 and 10 in M33. We contrasted our results with previous HMXB catalogs for both galaxies and with the classifications provided in the SIMBAD database. This last verification step revealed that several initial candidates were non-HMXB and were discarded from our search. The remaining sources form a clean sample for future studies. Our search allowed us to discover 12 new HMXB candidates that were not previously reported in the literature.
Keywords: High-mass X-ray binaries, M31, M33, Chandra, HST, catalogs
SDGs: Quality education

I. INTRODUCTION

High-mass X-ray binaries (HMXBs) are systems composed of a compact object and a massive companion star ($\geq 8\,M_\odot$) [13]. The compact object can either be a neutron star or a black hole, but the majority of known HMXBs contain a neutron star [7]. Because of its large mass relative to its small radius, the compact object generates an intense gravitational field, enabling it to accrete material from its companion star. There are two mechanisms by which the compact object can obtain material from the donor star, Roche lobe overflow (RLO) and stellar wind, but the dominant accretion mechanism in HMXBs is in most cases stellar wind: massive stars have powerful stellar winds with mass loss rates of $\geq 10^{-6}\,M_\odot\,yr^{-1}$, so direct wind accretion can result in relatively high accretion rates for binary separations of a few astronomical units (AU) or less [7].

The accreted material, due to the conservation of angular momentum, tends to form an accretion disk around the compact object. As the accreted material falls toward the compact object, its gravitational potential energy is converted into heat and light. This material reaches such a high temperature that its black-body emission peaks in the X-ray. X-ray binaries also emit radiation through three other mechanisms. These are Compton-up scattering, synchrotron radiation, and bremsstrahlung. The X-ray luminosity of HMXBs is in the range of $10^{35} - 10^{40}\,erg/s$ [7]. While X-ray radiation originates in the accretion disk, the optical counterpart of the system comes primarily from the massive donor star.

HMXBs are believed to generally form through the evolution of binary systems with two massive stars ($\geq 8\,M_\odot$) [22]. The star with the higher mass is the first to explode as a core-collapse supernova, compacting its core into a neutron star or a black hole. When the compact object starts accreting material from the companion star, the HMXB phase begins, and it is thought to last approximately 10^4 years [22]. Given their rapid formation times, the first generations of HMXBs may provide a substantial amount of X-ray heating to intergalactic gas during the Epoch of Reionization, impacting the onset and duration of this major phase transition in the early Universe [14], which is one of the major next frontiers in astrophysics [7]. The HMXB phase finishes when the donor star ends its life as a supernova, leaving behind a double compact object binary system or a disrupted system (depending on the supernova kick). Gravitational waves are produced as the orbit of a compact object binary shrinks, leading to a merger [1]. Understanding the formation and evolution of HMXBs therefore provides important insights into one of the primary formation channels of gravitational wave sources, an open question in the recent field of gravitational wave astrophysics [7].

The first HMXBs were detected around 1962 [9]. Six decades later, we have multiple extragalactic catalogs, for example, Williams et al. (2018) [32] and Lazzarini et al. (2021) [17] for M31, or Grimm et al. (2005) [11] and Lazzarini et al. (2023) [16] for M33.

Some of the extragalactic catalogs are outdated and do not include data from more recent observations (after 2023). This work will focus on exploring new potential candidates in M31 (Andromeda Galaxy) and M33 (Triangulum Galaxy), where new X-ray and optical data has been released since the last catalogs were published.

II. DATASETS

A. Chandra Source Catalog (CSC)

The Chandra Source Catalog (CSC) provides a comprehensive census of X-ray sources observed by the Chandra X-ray Observatory using its Advanced CCD Imaging Spectrometer (ACIS) and High Resolution Camera (HRC) [6]. The catalog provides positional, spatial, photometric, spectral, and temporal properties for each detected X-ray source. The photometric data provided by Chandra are fluxes in the ACIS broad band (b), which

corresponds to energies of $0.5-7.0$ keV, and in the HRC broad band (w) which corresponds to energies of $0.1-10$ keV. In this work we use the version 2.1 of the Chandra Source Catalog (CSC 2.1). This version includes 407,806 unique X-ray sources, identified in observations publicly released between January 2000 and December 2021 [6] (see Appendix A).

B. Heraklion Extragalactic Catalogue (HECATE)

The Heraklion Extragalactic Catalogue (HECATE) is an all-sky galaxy catalog that provides positions, sizes, distances, morphological classification, and astrophysical data for each galaxy. The catalog contains 204,733 galaxies within a distance of $D \leq 200$ Mpc [15]. In this work we use data from this catalog in order to identify the hosts of all nearby extragalactic Chandra X-ray sources. For this study focusing on X-ray binaries and their donor stars, since the stellar population of further galaxies can hardly be resolved, we restrict the sample to galaxies within a distance of $D \leq 20$ Mpc (see Appendix A).

C. Hubble Space Telescope (HST)

The Hubble Space Telescope (HST) is a large, space-based observatory that was launched in 1990. Since then, HST has been imaging targeted regions of the sky in wavelengths spanning ultraviolet to near infrared (115–2500 nanometers) [20]. To retrieve the HST sources, we use the data of Tranin et al. (2025) [27], making use of two databases comprising third-party catalogs in which source extraction has already been performed. The third release of the Hubble Source Catalog (HSCv3) [31] includes Advanced Camera for Surveys (ACS) and Wide-Field Camera 3 (WFC3) data that were public as of 2017 October 1. Later HST data were retrieved using Mikulski Archive for Space Telescopes (MAST) [21] queries with the `CasJobs` API [30]. The southern region of M31 has sparse coverage in HSCv3, but is well covered by more recent MAST catalogs. Tranin et al. (2025) [27] made sure that MAST catalogs are reliable and have well calibrated photometry, by comparing their sky coverage and their Color-Magnitude Diagram (CMD) with HSCv3 data. The photometric data we retrieve corresponds to filters F475W (green) and F814W (far red). To discard compact star clusters, cosmic rays and sources affected by confusion, we discarded sources with concentration indexes (CI) < 0.85 or > 1.5 or magnitude errors > 0.1 mag. The main use of this catalog in our work is finding optical counterparts for Chandra X-ray sources in both galaxies.

D. Gaia Data Release 3 (Gaia DR3)

Gaia Data Release 3 (Gaia DR3) provides astrometry and photometry for 1.8 billion sources brighter than magnitude 21 [8]. In this work we use Gaia DR3 astrometric data in order to filter and discard foreground contaminants from our sample, i.e. Milky Way stars.

III. DATA ANALYSIS

The first step in this work was to clean the data from the Chandra catalog, as broad band fluxes were missing for 67,698 sources. We then performed a crossmatch between Chandra and HECATE catalogs to identify the hosts of X-ray sources. The crossmatch was made using the "Sky Ellipses" algorithm in the `TOPCAT` software [26], where sources are matched if their associated ellipses overlap. The ellipse of each galaxy represents its extent (semi-major axis, semi-minor axis and position angle) while the ellipse of each X-ray source is taken to be its positional error ellipse. We took into account that Chandra X-ray point-sources have an uncertainty in position, but this uncertainty is small in comparison with the angular size of the galaxies we will be studying. We also discarded all sources in a radius of 2 arcsec around galactic nuclei positions provided by HECATE, with the main purpose of cutting possible Active Galactic Nuclei (AGN) in these galaxies. Figure 1 and Table I show the results of this crossmatch.

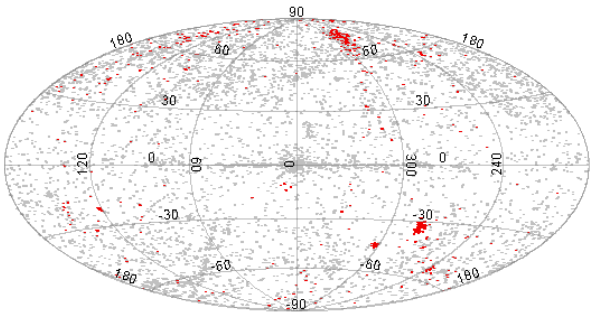

Figure 1: Aitoff projection of all CSC 2.1 X-ray sources in galactic coordinates (grey dots). In red are shown all the sources remaining after the crossmatch with HECATE.

Galaxy ID	X-ray sources
LMC	3239
SMC	2690
M 31	1518
M 33	734

Table I: Galaxies from HECATE catalog sorted by the number of Chandra X-ray point-sources they contain.

Table I shows the galaxies with most X-ray sources according to the crossmatch. We decided to discard the Large Magellanic Cloud (LMC) and Small Magellanic Cloud (SMC). The reason is that given their distance and extreme apparent size, HST has covered only a small fraction of these galaxies, making ground-based surveys better suited to study their stellar populations.

The following step was finding optical counterparts for M31 and M33 X-ray detections. To this end, we used HST data as described in Section II C. We then crossmatched the cleaned data with the Chandra X-ray

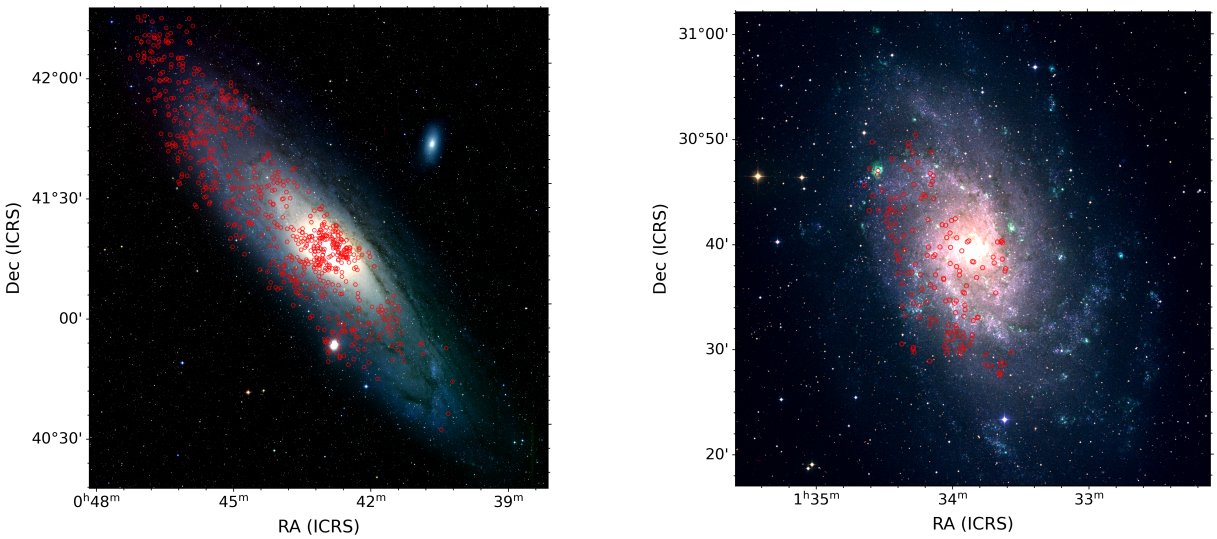

Figure 2: Resulting sources from the Chandra and HST crossmatch plotted on a RGB image for M31 (left) and M33 (right). The RGB images were made from IR, R and B fits from DSS2 [18], and they were plotted using `APLpy` `Python` module [24].

sources. This crossmatch was also done with `TOPCAT` [26], setting a maximum error radius of 1 arcsec. We obtained 733 matches for M31 and 155 for M33. The position of the resulting matches are shown in Figure 2 (see Appendix B).

To analyze the properties of HST sources in a CMD, we computed their Milky Way extinction-corrected absolute magnitude in F814W and their F475W−F814W color. Absolute magnitudes were calculated using Equation (1), where the distance modulus is based on the distance of the identified host, as reported in HECATE. Galactic extinctions for both filters and both galaxies were obtained using the NASA/IPAC Extragalactic Database (NED) [12]. With the broad band X-ray fluxes provided by Chandra we also calculated the X-ray luminosity of the sources using Equation (2).

$$M_F = m_F - 5\log_{10}(d_{Mpc}) - 25 - A_F \quad (1)$$

$$L_X = 4\pi \left(3.0857 \times 10^{24}\, d_{\mathrm{Mpc}}\right)^2 F_X \quad (2)$$

Having obtained absolute magnitudes for both the F475W and F814W filters, we plotted the CMDs for both galaxies (Figure 3). We overlaid the modeled evolutionary tracks of single stars of different masses, retrieved via the MIST website [3]. Since MIST requires a metallicity value to generate evolutionary tracks, we adopted [Fe/H] = −0.023 for M31 [10] and [Fe/H] = −0.078 for M33 [4].

Since our focus lies on HMXBs, we excluded all sources below the $6\,M_\odot$ curve. While this is lower than the $8\,M_\odot$ threshold used to define HMXBs (Section I), we decided to allow a margin because we do not know the extinction that the sources actually have inside M31 and M33 galaxies, so these stars could be more massive than they appear to be. After this cut, there were 26 sources remaining for M31 and 12 for M33.

At this stage of the analysis, the sample still contained MW foreground star contaminants, aligning with M31 and M33 by chance. To identify and exclude such sources, we crossmatched the sample to Gaia DR3 using a matching radius of 1 arcsec. Unlike extragalactic sources, MW stars have significant parallaxes and proper motions (PM) in Gaia. We therefore flagged as contaminant and discarded any source having a parallax ten times larger than its error, or a PM five times larger than its error. After this last crossmatch, there are 18 remaining sources for M31, shown in Table II, and 10 remaining sources for M33, shown in Table III.

Using the `Python` module `ztfquery` [23], we obtained light curves from the Zwicky Transient Facility (ZTF) archive at IRSA [2] for all the sources in our final sample. We analyzed these light curves with the non parametric kernel regression method for optimal optical frequency determination `FINKER` [25] to search for periodic signals. However, no significant periodicity was detected in any source.

IV. RESULTS AND DISCUSSION

After applying all the selection criteria described in Section III, we obtained the final sample of HMXB candidates for both galaxies. This sample comprises 18 sources in M31 (Table II) and 10 sources in M33 (Table III). We also plot the CMD of the candidates for both galaxies in Figure 3.

To verify our findings, we compared our candidates with existing HMXB catalogs for the same galaxies. To this end, we crossmatched the M31 candidates with the Williams et al. (2018) [32] and Lazzarini et al. (2021) [17] catalogs, and the M33 candidates with the Lazzarini et al. (2023) catalog. We also verified each candidate in the SIMBAD database [29] to identify any previously cata-

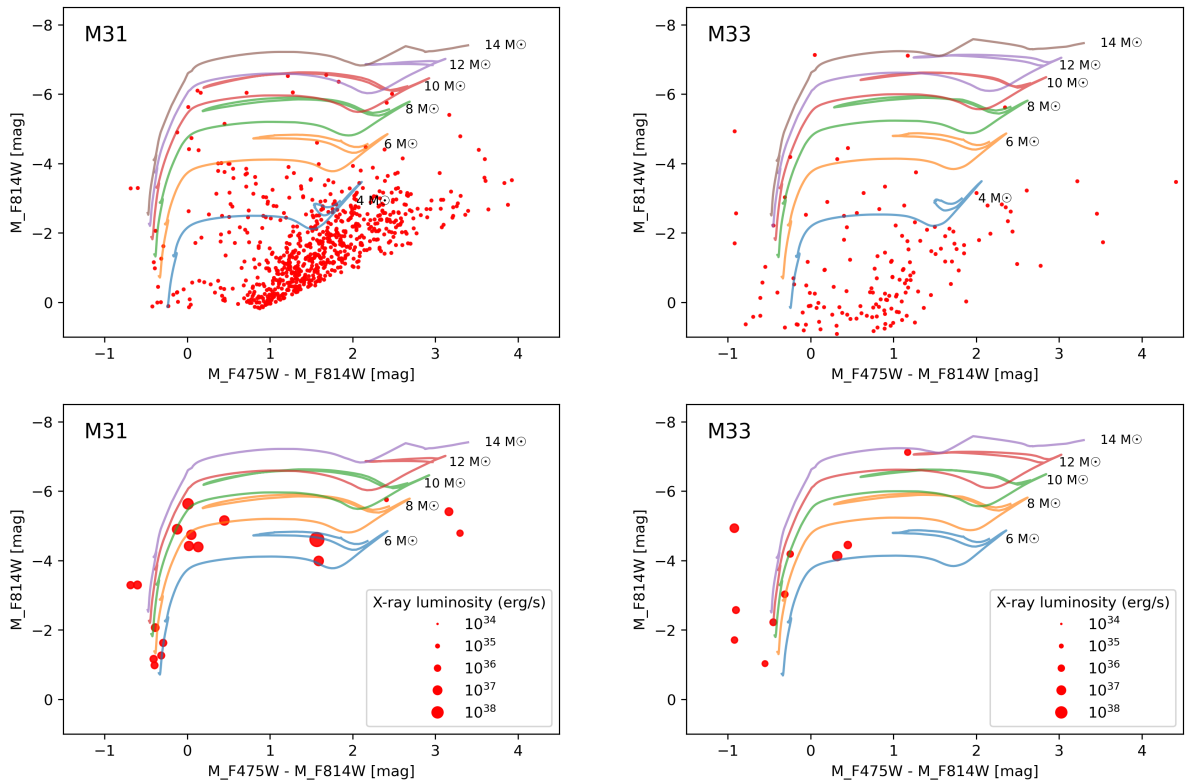

Figure 3: CMDs for all M31 crossmatched sources (top-left), all M33 crossmatched sources (top-right), M31 final candidates (bottom-left) and M33 final candidates (bottom-right). The x-axis represents the source color using extinction-corrected F475W and F814W filters. The y-axis shows the extinction-corrected absolute magnitude in the F814W filter. For final candidates, symbol sizes scale with their broad band X-ray luminosity. We overlay evolutionary tracks for stars of mass in the range $4 - 14\,M_\odot$ obtained from MIST [3].

Name 2CXO	RA (deg)	Dec (deg)	L_X (erg/s)	M_{F475W} (mag)	M_{F814W} (mag)
J004013.8+405004	10.0575	40.8346	4.33×10^{38}	−3.038	−4.605
J004115.3+410102	10.3140	41.0174	3.18×10^{36}	−4.695	−4.742
J004126.1+405326	10.3592	40.8907	4.48×10^{36}	−5.026	−4.903
J004137.9+410107	10.4080	41.0188	3.35×10^{36}	−4.707	−5.155
J004154.9+405714	10.4791	40.9539	2.64×10^{35}	−1.378	−0.981
J004207.9+410436	10.5330	41.0769	4.33×10^{36}	−4.260	−4.392
J004231.1+410435	10.6301	41.0765	2.88×10^{36}	−4.400	−4.419
J004232.7+411648	10.6366	41.2802	6.65×10^{35}	−2.245	−5.408
J004235.0+404839	10.6458	40.8109	1.05×10^{37}	−5.626	−5.634
J004242.8+405512	10.6785	40.9199	8.89×10^{33}	−3.344	−5.752
J004247.0+411910	10.6962	41.3197	1.30×10^{35}	−1.491	−4.789
J004311.6+410605	10.7989	41.1016	5.87×10^{35}	−2.456	−2.067
J004404.7+412127	11.0197	41.3576	3.81×10^{36}	−2.400	−3.989
J004420.1+413407	11.0840	41.5689	3.25×10^{35}	−1.919	−1.627
J004441.6+412959	11.1736	41.4998	2.71×10^{35}	−1.579	−1.263
J004514.6+415038	11.3115	41.8429	6.92×10^{35}	−3.900	−3.296
J004637.2+421034	11.6551	42.1762	3.55×10^{35}	−3.979	−3.292
J004645.2+420611	11.6888	42.1031	3.56×10^{35}	−1.570	−1.162

Table II: M31 HMXB candidates

Name 2CXO	RA (deg)	Dec (deg)	L_X (erg/s)	M_{F475W} (mag)	M_{F814W} (mag)
J013356.7+303729	23.4865	30.6249	3.36×10^{36}	−3.809	−4.129
J013358.9+303426	23.4957	30.5739	1.74×10^{35}	−3.340	−3.027
J013402.4+304040	23.5102	30.6779	1.08×10^{35}	−5.948	−7.119
J013402.8+304151	23.5120	30.6976	1.45×10^{36}	−5.855	−4.933
J013403.7+303641	23.5155	30.6116	8.46×10^{34}	−1.581	−1.029
J013417.0+303426	23.5713	30.5740	4.15×10^{35}	−4.000	−4.448
J013417.1+304843	23.5715	30.8122	2.17×10^{35}	−2.674	−2.222
J013417.2+303004	23.5721	30.5012	1.49×10^{35}	−2.630	−1.709
J013421.2+304334	23.5886	30.7262	1.45×10^{35}	−4.437	−4.189
J013432.7+304704	23.6366	30.7844	2.45×10^{35}	−3.476	−2.573

Table III: M33 HMXB candidates

loged objects from earlier studies. Finally, we performed a visual verification using the ESASky astronomical visualization tool [19].

Williams et al. (2018) catalog provides HST optical magnitudes for 57 HMXB candidates in M31, while Lazzarini et al. (2021) reports additional stellar parameters for the same 57 sources. Both catalogs are restricted to the northern region of M31, where only the last 6 of our 18 final candidate sources are located. A preliminary crossmatch yields 54 common sources before application of our selection criteria, but only three candidates (J004420.1+413407, J004514.6+415038, and J004637.2+421034) satisfy all the cuts described in Section III. The significant reduction in matching sources primarily comes from the removal of low-mass stars below $6\,M_\odot$, which excludes 50 candidates from the catalog. An additional source is rejected in the foreground contamination filtering. Notably, when taking the Williams

et al. (2018) photometric data directly, 13 sources satisfied our mass threshold, despite both studies using HST optical data. A probable reason for this discrepancy is the fact that they are using HST photometry that has been corrected using extinction map of dust clouds in M31 [5], while we only corrected for MW extinction.

The Lazzarini et al. (2023) catalog contains 65 HMXB candidates in M33, generated through a cross-matching between X-ray sources from ChASeM33 [28] and HST optical observations. Unlike M31, Lazzarini et al. (2023) have wider optical coverage in M33 than us, excluding 35 of their sources from our analysis due to field limitations. In M33, we initially identified 30 sources in common with Lazzarini et al. (2023). After applying our selection criteria, five out of ten candidates remain in our final sample: J013356.7+303729, J013402.8+304151, J013417.0+303426, J013417.1+304843, and J013421.2+304334. Notably, using their optical photometry we obtained the same candidates in our HST data field.

The SIMBAD database verification reveals several previously classified objects in the candidate list. For M31, the source J004013.8+405004 was confirmed as a BL Lacertae object, both J004126.1+405326 and J004137.9+410107 were recognized as quasars, J004232.7+411648 was classified as a classical nova, and J004404.7+412127 was cataloged as a variable star. For M33, both J013358.9+303426 and J013417.0+303426 were classified as supernova remnants (SNR), J013402.4+304040 was identified as a globular cluster and J013432.7+304704 was cataloged as a Wolf-Rayet system.

Performing the visual inspection with the ESASky tool we noticed that there is no detectable Chandra X-ray source at the position of the M31 candidate J004441.6+412959, which is also flagged as variable. This suggests that J004441.6+412959 could be a transient object.

V. CONCLUSION

This study identified 18 HMXB candidates in M31 and 10 in M33 by combining Chandra X-ray data with HST optical observations. Rigorous selection criteria, including mass cuts ($\geq 6\,M_\odot$), Gaia DR3 foreground contamination filtering, and SIMBAD verification, ensured a reliable sample. When comparing with reference catalogs for both galaxies we recovered part of their HMXB candidates. This work demonstrates the need for updated multi-wavelength HMXB searches. Future observations could confirm these candidates.

VI. ACKNOWLEDGMENTS

I would like to thank my advisors, Nadejda Blagorodnova and Hugo Tranin, for the support they have given me during this project. They have guided me excellently through all its stages, and thanks to them I have learned to navigate the world of astrophysical research better. I would also like to thank my family for the support they have given me during the most difficult moments.

[1] Belczynski, K., Kalogera, V., & Bulik, T. 2002, Astrophys. J. , 572, 407
[2] Bellm, E. C., et al. 2019, PASP, 131, 018002
[3] Choi, J., et al. n.d., MIST, `https://waps.cfa.harvard.edu/MIST/`
[4] Cioni, M. R. L. 2009, A&A, 506, 1137
[5] Dalcanton, J. J., et al. 2015, Astrophys. J. , 814, 3
[6] Evans, I. N., et al. 2024, ApJS, 274, 22
[7] Fornasini, F. M., Antoniou, V., & Dubus, G. 2023, High-mass X-ray Binaries
[8] Gaia Collaboration, et al. 2023, A&A, 674, A1
[9] Giacconi, R., et al. 1962, Phys. Rev. Lett. , 9, 439
[10] Gibson, B. J., et al. 2023, Astrophys. J. , 952, 23
[11] Grimm, H. J., et al. 2005, ApJS, 161, 271
[12] Helou, G., et al. 1995, in Information & On-Line Data in Astronomy, ed. D. Egret & M. A. Albrecht, Vol. 203, 95
[13] Hunt, Q., et al. 2021, Astrophys. J. , 912, 31
[14] Jeon, M., et al. 2014, Monthly Notices of the Royal Astronomical Society, 440, 3778–3796
[15] Kovlakas, K., et al. 2021, MNRAS, 506, 1896
[16] Lazzarini, M., et al. 2023, Astrophys. J. , 952, 114
[17] Lazzarini, M., et al. 2021, Astrophys. J. , 906, 120
[18] McLean, B. J., et al. 2000, in Astronomical Society of the Pacific Conference Series, Vol. 216, Astronomical Data Analysis Software and Systems IX, ed. N. Manset, C. Veillet, & D. Crabtree, 145
[19] Merín, B., et al. 2015, ESA Sky: a new Astronomy Multi-Mission Interface
[20] NASA. n.d., About Hubble, `https://science.nasa.gov/mission/hubble/overview/about-hubble/`
[21] NASA. n.d., Mikulski Archive for Space Telescopes, https://archive.stsci.edu/
[22] Postnov, K. A. & Yungelson, L. R. 2014, Living Reviews in Relativity, 17, 3
[23] Rigault, M. 2018, ztfquery, a python tool to access ZTF data
[24] Robitaille, T. 2019, APLpy v2.0: The Astronomical Plotting Library in Python
[25] Stoppa, F., et al. 2024, A&A, 686, A158
[26] Taylor, M. 2011, TOPCAT: Tool for OPerations on Catalogues And Tables, Astrophysics Source Code Library, record ascl:1101.010
[27] Tranin, H., et al. 2025, Astronomy & Astrophysics, 695, A226
[28] Tüllmann, R., et al. 2011, ApJS, 193, 31
[29] Wenger, M., et al. 2000, A&AS, 143, 9
[30] White, R. & Necker, J. n.d., mastcasjobs, `https://github.com/rlwastro/mastcasjobs`
[31] Whitmore, B. C., et al. 2016, AJ, 151, 134
[32] Williams, B. F., et al. 2018, ApJS, 239, 13

Descobrint estrelles binàries de raigs X d'alta massa extragalàctiques

Author: Marc Miguel Rivas, mmigueri11@alumnes.ub.edu
Facultat de Física, Universitat de Barcelona, Diagonal 645, 08028 Barcelona, Spain.

Advisors: Nadejda Blagorodnova, nblagorodnova@ub.edu; Hugo Tranin, htranin@icc.ub.edu

Resum: Aquest TFG presenta una recerca d'estrelles binàries de raigs X d'alta massa (HMXB) a les galàxies M31 i M33 utilitzant dades de raigs X de Chandra i dades òptiques del Hubble Space Telescope (HST). La nostra selecció creua les dues bases de dades, aplica un criteri de tall basat en la massa estel·lar i elimina la contaminació de fonts galàctiques coincidents en posició amb M31 i M33. Això ens permet identificar 18 objectes candidats a HMXB a M31 i 10 a M33. Hem contrastat els nostres resultats amb catàlegs previs d'HMXB per a ambdues galàxies i amb la base de dades SIMBAD. Tot i que diversos candidats inicials a HMXB van ser reclassificats com a altres objectes astrofísics mitjançant la verificació a SIMBAD, les fonts restants conformen una mostra útil per a futurs estudis. La nostra recerca ens ha permès descobrir 12 nous candidats a HMXB que no estaven presents en la literatura.
Paraules clau: Estrelles binàries de raigs X d'alta massa, M31, M33, Chandra, HST, catàlegs
ODSs: Educació de qualitat

Objectius de Desenvolupament Sostenible (ODSs o SDGs)

1. Fi de les desigualtats		10. Reducció de les desigualtats	
2. Fam zero		11. Ciutats i comunitats sostenibles	
3. Salut i benestar		12. Consum i producció responsables	
4. Educació de qualitat	X	13. Acció climàtica	
5. Igualtat de gènere		14. Vida submarina	
6. Aigua neta i sanejament		15. Vida terrestre	
7. Energia neta i sostenible		16. Pau, justícia i institucions sòlides	
8. Treball digne i creixement econòmic		17. Aliança pels objectius	
9. Indústria, innovació, infraestructures			

Table IV: Objectius de Desenvolupament Sostenible (ODSs o SDGs)

El contingut d'aquest TFG, part d'un grau universitari de Física, es relaciona amb l'ODS 4, i en particular amb la fita 4.4, ja que contribueix a l'educació a nivell universitari.

Appendix A: Datasets

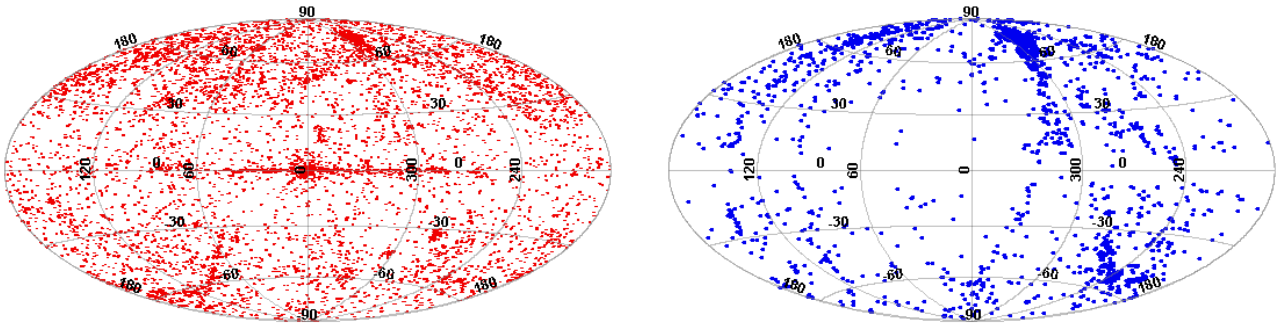

Figure 4: Aitoff projection of all CSC 2.1 X-ray sources (left) and all HECATE galaxies at distance $\leq$ 20 Mpc (right), both in Galactic coordinates.

Appendix B: Crossmatches

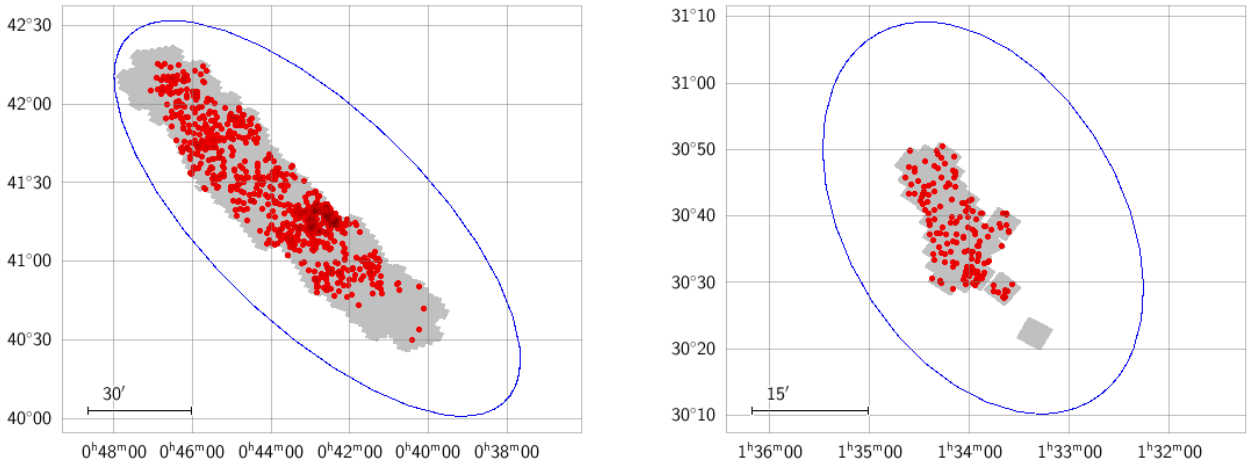

Figure 5: Resulting sources from the Chandra and HST crossmatch for M31 (left) and M33 (right). Gray regions show the area covered by our optical HST data, while red points mark the positions of matched sources. Blue ellipses show the size of each galaxy provided by HECATE.